Eur. Phys. J. B **24**, 143–147 (2001)

THE EUROPEAN PHYSICAL JOURNAL B

EDP Sciences

EPR study of Dy^{3+} ions in $DyBa_2Cu_3O_{6+x}$

V. Likodimos[1], N. Guskos[2,3], J. Typek[3,a], and M. Wabia[3]

[1] Department of Applied Mathematics and Physics, National Technical University, 157 80 Athens, Greece
[2] Solid State Section, Department of Physics, University of Athens, 157 84 Zografos, Panepistimiopolis, Athens, Greece
[3] Institute of Physics, Technical University of Szczecin, Al. Piastow 17, 70 310 Szczecin, Poland

Received 3 June 2001

Abstract. Concentrated polycrystalline $DyBa_2Cu_3O_{6+x}$ compounds are studied by X-band EPR spectroscopy. A broad resonance line due to the highly anisotropic EPR spectrum of Dy^{3+} ions is identified on several specimens at low temperatures. Powder simulation of the EPR spectra complies with the ground Kramers doublet predicted by crystal field analysis of Dy^{3+} ions. Calculations of the second and fourth moments of the resonance lines due to the dipole-dipole interactions of Dy^{3+} indicate the presence of substantial exchange narrowing of the dipolar-broadened EPR linewidth.

PACS. 76.30.-v Electron paramagnetic resonance and relaxation – 74.70.-b Superconducting materials (excluding high-T_c compounds)

1 Introduction

A considerable wealth of experimental studies has been devoted in the investigation of rare earth (R) magnetism coexisting with high-T_c superconductivity in the $RBa_2Cu_3O_{6+x}$ (R123) layered compounds [1,2]. Thorough investigations have shown that the low-temperature ordered states of the R^{3+} sublattice are mainly determined by the interplay between the long-range dipolar interaction and the short-range exchange interaction, which varies substantially along the lanthanide series and most importantly as a function of the oxygen doping [1–4].

Electron paramagnetic resonance (EPR) studies of rare earth-doped high-T_c superconductors have provided valuable information on the ground state properties of R^{3+} ions [5], which have been further employed as sensitive probes of spin dynamics in high-T_c superconductors [6]. EPR spectroscopy in concentrated R123 compounds has been exploited to clarify the origin of the exchange coupling between R^{3+} ions and to provide an independent estimate of its magnitude through the analysis of the EPR linewidth [7–9]. In both cases, however, the application of EPR has been mainly focused on the S-state Gd^{3+} ions and to a lesser extent on the heavier Er^{3+} and Yb^{3+} Kramers ions, while recently the observation of the low field EPR spectrum for Dy^{3+} ions in oxygen-deficient Y123 has been reported [10].

To elucidate the origin of the EPR spectra and verify the presence of exchange coupling between Dy^{3+} ions, we have carried out an X-band EPR study on concentrated $DyBa_2Cu_3O_{6+x}$ compounds subjected to different thermal treatments. The EPR spectrum due to Dy^{3+} ions is observed at low temperatures, in accord with the large anisotropy of the ground Kramers doublet predicted by crystal field analysis. Although the Dy^{3+} EPR spectrum is excessively broadened in the X-band, comparison with the EPR linewidth due to the dipolar interaction provides strong evidence for the presence of exchange narrowing.

2 Experimental details

EPR measurements were performed on polycrystalline $DyBa_2Cu_3O_{6+x}$ samples derived from the corresponding single-phase Dy123 high-T_c superconductors, which were earlier prepared by the standard solid state reaction technique [11]. Partial deoxygenation of the samples was carried out by thermal treatment in He atmosphere at 850 °C followed by rapid cooling at room temperature in the reducing atmosphere. The EPR spectra were recorded on fine powder samples, sealed in quartz tubes, using an X-band ($\nu = 9.43$ GHz) Bruker 200D spectrometer at various time intervals after the final thermal treatment. The magnetic field was scaled with an NMR magnetometer. An OXFORD flow-cryostat was employed for measurements in the temperature range of 4.2–20 K.

3 Results and discussion

Figure 1 shows the low temperature EPR spectra at variable microwave power for an "aged" Dy123 superconductor and the corresponding oxygen-deficient sample obtained after thermal treatment in He atmosphere at

[a] e-mail: typjan@arcadia.tuniv.szczecin.pl

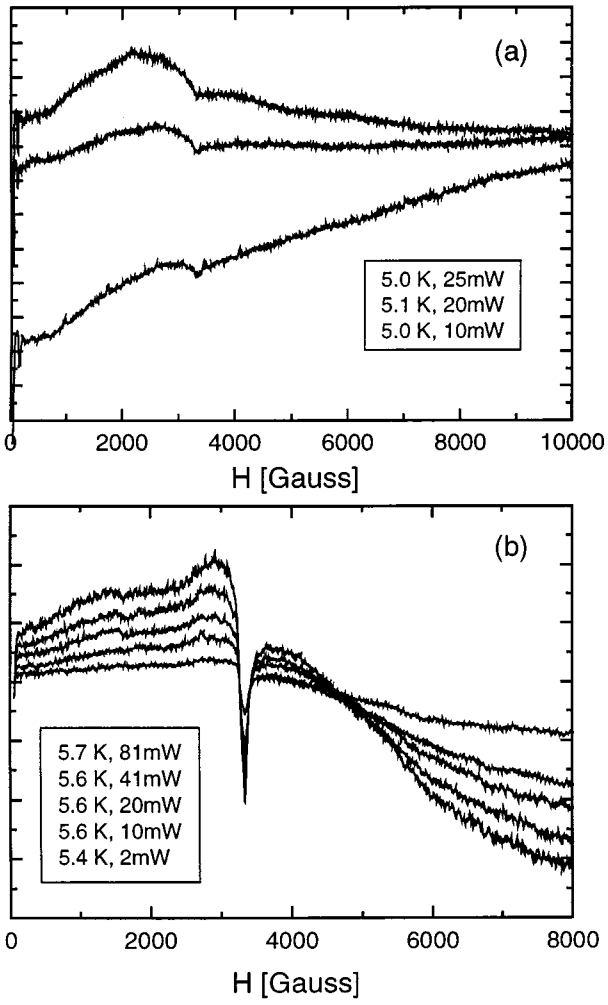

Fig. 1. Low temperature X-band EPR spectra of polycrystalline $DyBa_2Cu_3O_{6+x}$ compounds at increasing microwave power. (a) Fully oxygenated, "aged" superconducting sample and (b) partially deoxygenated sample.

850 °C for 24 h. At low microwave power, a weak signal with some complex structure is observed near zero magnetic field in the superconducting sample (Fig. 1a) and a rather weak $g \approx 2.0$ EPR signal due to Cu^{2+} paramagnetic defect centers, which is more clearly detected on the oxygen deficient phase (Fig. 1b). The former signal resembles closely the anomalous non-resonant microwave absorption most frequently detected in degraded high-T_c superconductors [12]. In the oxygen-deficient sample (Fig. 1b), a very weak $g \approx 4.2$ resonance line becomes gradually resolved along with the intense Cu^{2+} anisotropic EPR powder spectrum, which may be due to the presence of a low concentration of copper pairs or even iron impurities. However, the most interesting feature of the EPR spectra at higher microwave power, is the observation of a very broad, asymmetric EPR spectrum, most prominent in the oxygen deficient sample (Fig. 1b). This EPR spectrum appears to be shifted at high resonance fields and stems from the resonance spectrum of Dy^{3+} as will be shown below.

To verify the latter observation, further EPR measurements were performed on another polycrystalline Dy123 sample. Figure 2a shows the EPR spectra recorded immediately after the thermal treatment of the sample in He atmosphere at 850 °C for 2 h. In this case, only the anisotropic $g \approx 2.0$ EPR spectrum and the $g \approx 4.2$ EPR lines were observed along with some very weak fine structure lines due to molecular oxygen contamination [13], superimposed on a very broad background line. Subsequent measurements on the same Dy123 sample one month and two months after its thermal treatment are shown in Figures 2b and 2c, respectively. In both cases, the broad EPR spectrum can be clearly evinced spanning over the entire magnetic field range. A weak signal is also observed at very low fields, most probably due to the non-resonant microwave absorption that indicates a very small superconducting volume fraction characterizing the partly deoxygenated state of the present samples. It is also worth noting the appearance of an intense EPR spectrum in $g \approx 2.2$ region, which becomes progressively separated from the persistent Cu^{2+} EPR pattern with the passage of time. The latter EPR spectrum, which shifts towards lower magnetic fields and exhibits a non-monotonic temperature variation of its intensity is indicative of the formation of metastable copper complexes such as copper pairs or other paramagnetic centers due to exchange coupled copper ions with antiferromagnetic ground states [14].

Despite the excessively large linewidth in the X-band, the broad EPR spectrum can be consistently attributed to the EPR spectrum of Dy^{3+} ions. The crystal field (CF) interaction of Dy^{3+} ($4f^9$) has been studied by inelastic neutron scattering in the Dy123 superconductor [15]. The CF parameters for the corresponding D_{2h} site-symmetry were derived, in the context of Stevens formalism, by fitting the four lowest excited CF states that were experimentally determined. In this case, the 16-fold degenerate $^6H_{15/2}$ ground term of Dy^{3+} is split into eight Γ_5 Kramers doublets. According to the crystal field analysis, the ground state wavefunction comprises a dominant (≈98%) contribution of the $M = \pm 11/2$ component with principal g-values $g_x = 1.8$, $g_y = 1.2$ and $g_z = 14.2$, implying Ising-like anisotropy [15]. Table 1 shows the corresponding CF parameters, converted in the spherical tensor formalism [16], in comparison with some representative values reported for the heavier R^{3+} ions in the R123 crystal structure [17–23], as well as the CF parameters predicted for Dy^{3+} by the superposition model analysis [24]. As can be seen in Table 1, the values of the leading fourth and sixth order CF parameters for Dy^{3+} are systematically smaller than the values reported for the other R^{3+} ions for which a smooth reduction following the lanthanide contraction would be expected.

To explore the latter behavior and its implication on the ground state properties of Dy^{3+}, we have calculated the crystal field energy levels in the spherical tensor operator formalism using the two lowest J multiplets of Dy^{3+} with intermediate coupling wavefunctions [25] and allowing for J-mixing. Good agreement with the experimental energy levels (0, 3.3 ± 0.1, 5.9 ± 0.2, 14.0 ± 0.5 and

Table 1. Crystal field parameters (in cm^{-1}) in the spherical tensor formalism for R^{3+} ions in the D_{2h} site symmetry of $RBa_2Cu_3O_{6+x}$ (R123) ($x \approx 1$) high-T_c superconductors.

	B_2^0	B_2^2	B_4^0	B_4^2	B_4^4	B_6^0	B_6^2	B_6^4	B_6^6	Ref.
Dy123	261	33	–1547	59	885	253	–5.4	618	3.6	[15]
	339	33	–1670	59	928	298	–5.6	686	5.4	this work
	-	-	–2140	124	1205	671	–1	1404	2.0	[24]
Ho123	331	57	–1766	16	976	452	–24	1202	–10.0	[17]
	435	77	–1907	–297	1050	472	–253	1305	–15.0	[18]
	548	–48	–2065	–113	1040	484	–40	1307	24.0	[19]
Er123	324	150	–1942	–4	1338	458	–56	1237	0.0	[20]
	225	77	–2081	105	1209	474	–7	1202	5.4	[21]
Tm123	372	112	–1856	119	1134	432	–168	1263	0.0	[22]
Yb123	92	13	–2088	82.5	1152	576	–8	1259	5.7	[23]

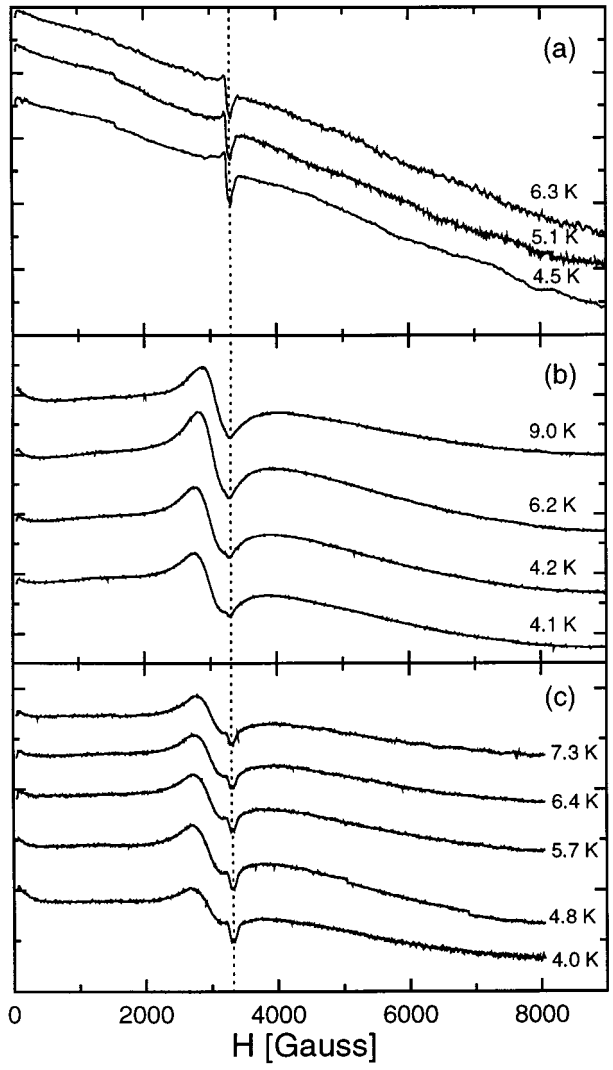

Fig. 2. Low temperature X-band EPR spectra of an oxygen-deficient $DyBa_2Cu_3O_{6+x}$ sample at various time intervals after thermal treatment. (a) Fresh sample, (b) 1 month and (c) 2 months after thermal treatment. The dotted line indicates the constant position of the Cu^{2+} EPR spectrum.

17.0 ± 1 meV [15]) was obtained for the set of CF parameters shown in the second row of Table 1. The calculated energy levels are found at 0, 3.28, 5.70, 14.31 and 17.39 meV, while the corresponding ground doublet is still dominated by the $M = \pm 11/2$ component (≈99%) resulting in the even more anisotropic g-values $g_x = 0.86$, $g_y = 0.78$ and $g_z = 14.17$. The derived CF parameters are indeed larger than those previously determined for Dy^{3+} though they remain smaller than those reported the other R^{3+} ions (Tab. 1), indicative for the need of further refinement of the CF parameters based on a wider experimental CF energy spectrum [26].

Powder simulation of the Dy^{3+} EPR spectrum was subsequently performed for the corresponding ground doublet, which is described by an effective spin $S = 1/2$, based on the calculated g-values. Reasonably good agreement with the broad experimental EPR spectrum was obtained for axial g-anisotropy with $g_\parallel \approx 14.0$ and $g_\perp \approx 1.0$ and anisotropic linewidths of magnitude $\Delta H_\parallel \approx 4500$ Gs and $\Delta H_\perp \approx 1000$ Gs, in magnetic field units. Simulated EPR spectra in comparison with the experimental ones are shown in Figure 3. Comparison with the EPR spectra of c-axis aligned $Y_{0.99}Dy_{0.01}Ba_2Cu_3O_6$ polycrystalline samples, where $g_\parallel$ values of 11.5 and 7.0 have been determined for the ground and first excited CF doublets, respectively [10], is not presently feasible as the $g_\parallel$ component of the powder EPR spectrum could not be reliably determined with the present spectral resolution. Moreover, due to the large resonance width that strongly exceeds the resonance field H_r, absorption at both $\pm H_r$ caused by the two oppositely rotating components of the linearly polarized rf field, which were not taken into account in the powder simulation, may give an appreciable contribution in the EPR spectrum, especially in the lower field region ($H < 3000$ G). Further analysis shows that the broad EPR spectra may be also fitted to a reasonable approximation with a single Lorentzian line including both circularly polarized components, the largest deviation occurring in the low field region, with g-values in the range of 1.32–1.42 and isotropic linewidth $\Delta H \approx 7600(100)$ Gs. The latter results were subsequently explored to obtain a

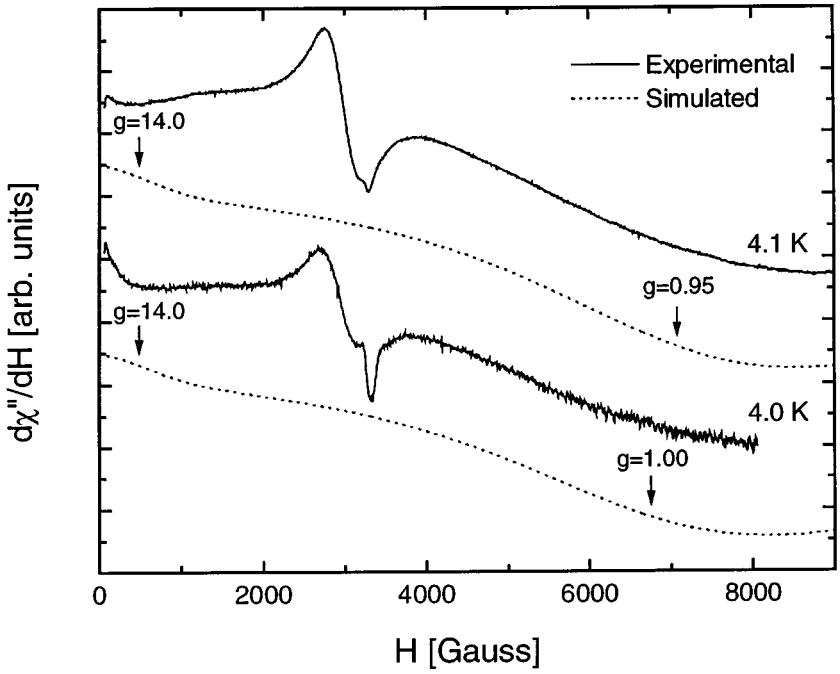

Fig. 3. Simulated X-band (ν = 9.4358 GHz) EPR spectra of Dy^{3+} ions in comparison with the experimental ones at low temperature. The simulation was performed for $S = 1/2$ with axially symmetric g-tensor, Lorentz lineshape function and anisotropic linewidth (half-width at half-height) with $g_{\|} = 14.0$, $g_{\perp} = 0.95$, $\Delta H_{\|} = 4400$ Gs, $\Delta H_{\perp} = 1000$ Gs (upper curve) and $g_{\|} = 14.0$, $g_{\perp} = 1.0$, $\Delta H_{\|} = 4500$ Gs, $\Delta H_{\perp} = 1000$ Gs (lower curve).

rough estimate of the EPR intensity and the corresponding spin concentration by comparison to $CuSO_4 \cdot 5H_2O$. For the EPR spectrum corresponding to the Dy123 sample one month after its thermal treatment (Fig. 2b), the spin concentration is found, within at least 50% error mainly caused by the linewidth uncertainty, to approach the nominal Dy^{3+} concentration in the Dy123 host. However, an appreciable reduction of the spin concentration, approximately by an order of magnitude, is estimated after further time exposition (Fig. 2c). Considering that the Dy^{3+} EPR spectrum nearly vanishes immediately after thermal treatment (Fig. 2a), more accurate investigations of the temporal evolution of the EPR intensity might be a useful probe of oxygen rich regions during the aging process. Despite these shortcomings, it can be clearly evinced that the broad X-band EPR spectrum, systematically observed in concentrated Dy123 compounds, stems from the anisotropic powder spectrum of Dy^{3+} ions with a dominant contribution from the high field $g_{\perp}$ component.

To explore further the broadening of the Dy^{3+} EPR spectrum, the dipolar EPR linewidth of Dy^{3+} ions in the Dy123 crystal structure was analyzed employing the method of moments [8,9]. The secular second $M_2^{(0)}$ and fourth $M_4^{(0)}$ moments due to the dipole-dipole interaction as a function of the angle θ of H with the c-axis were accordingly calculated in the high-temperature approximation. An axial g-tensor with principal values $g_{\|} \approx 14.0$ and $g_{\perp} \approx 1.0$ was explicitly taken into account, while the implicated lattice sums were numerically calculated within $7a \times 7a$ block in ab plane with lattice constant $a = b = 3.860$ Å. The secular moments, parallel and perpendicular to the c-axis, are found to be $M_{2\|}^{(0)} \approx 22.9 \times 10^8$ (MHz)^2, $M_{4\|}^{(0)} \approx 136.2 \times 10^{17}$ (MHz)^4 and $M_{2\perp}^{(0)} \approx 5.7 \times 10^8$ (MHz)^2, $M_{4\perp}^{(0)} \approx 8.5 \times 10^{17}$ (MHz)^4 and the corresponding values of the ratio $\mu = M_2^{(0)}/M_4^{(0)}$ are $\mu_{2\|} = 2.60$ and $\mu_{2\perp} = 2.61$, close to the value of $\mu = 3$ expected for Gaussian lineshape function [27]. The dipolar EPR linewidth (half-width at half height) would be then given by $\Delta H_i = \sqrt{2 \ln 2}\sqrt{M_{2i}^{(0)}}$ leading to the anisotropic values of $\Delta H_{\|} \approx 2900$ Gs and $\Delta H_{\perp} \approx 20100$ Gs, in magnetic field units.

Comparison of the linewidth values derived from the simulation ($\Delta H_{\|} \approx 4500$ Gs and $\Delta H_{\perp} \approx 1000$ Gs) with the theoretical dipolar widths shows that the experimental EPR spectrum is much narrower on both principal directions. Even though the linewidth values of the Dy^{3+} EPR spectrum may be only a rough approximation due to the limited spectral resolution in X-band, the latter result provides strong evidence for the presence of substantial exchange narrowing. Moreover, another contribution to the EPR linewidth might be inferred from the presence of a rapidly fluctuating internal field [28] that has been recently related to the orbital magnetic state that may be pertinent to the inhomogeneous superconducting phase of most high-T_c cuprates [29,30].

Accurate determination of the anisotropic linewidth at higher EPR frequencies would further enable a quantitative estimate of the exchange coupling between Dy^{3+}

ions, which, according to the theoretical treatment of the specific heat data, varies considerably as a function of the oxygen content [1] and the investigation of additional contributions to the relaxation rate of Dy^{3+} ions.

4 Conclusions

The anisotropic EPR spectrum of Dy^{3+} ions is identified in concentrated $DyBa_2Cu_3O_{6+x}$ compounds subjected to different thermal treatments employing X-band EPR measurements. The EPR spectrum due to Dy^{3+} ions comprises a broad asymmetric resonance line due to the dominant contribution of the high field $g_\perp$ component of the corresponding powder EPR pattern, which complies with the crystal field ground doublet. Comparison of the theoretical dipolar width with the experimental EPR spectrum indicates the presence of exchange narrowing.

References

1. P. Allenspach, M.B. Maple, in *Handbook on the Physics and Chemistry of the Rare Earths*, edited by K.A. Gschneider, L. Eyring, M.B. Maple, Vol. **22** (Amsterdam, North-Holland, 1998).
2. T.W. Clinton, J.W. Lynn, J.Z. Liu, Y.X. Jia, T.J. Goodwin, R.N. Shelton, B.W. Lee, M. Buchgeister, M.B. Maple, Phys. Rev. B **51**, 15429 (1995).
3. S.K. Misra, J. Felsteiner, Phys. Rev. B **46**, 11033 (1992).
4. A.B. MacIsaak, J.P. Whitehead, K. de Bell, K.S. Narayanan, Phys. Rev. B **46**, 6387 (1992).
5. S.K. Misra, Y. Chang, J. Felsteiner, J. Phys. Chem. Solids **58**, 1 (1997).
6. C.S. Sunandana, in *Studies of High Temperature Superconductors*, Vol. **29** (Nova Science Publishers, New York, 1999), p. 187.
7. C. Fillip, C. Kessler, F. Balibanu, P. Kleeman, A. Darabont, L.V. Giurgiu, M. Mehring, Physica B **222**, 16 (1996).
8. V. Likodimos, N. Guskos, M. Wabia, J. Typek, Phys. Rev. B **58**, 8244 (1998).
9. V. Likodimos, N. Guskos, H. Gamari-Seale, M. Wabia, J. Typek, Phys. Rev. B **58**, 14223 (1998).
10. M.R. Gafurov, V.A. Ivanshin, I.N. Kurkin, M.P. Rodionova, H. Keller, M. Guttman, *International Conference on Magnetic Resonance and Related Phenomena, 29th AMPERE-13th ISMAR, Berlin, August 2-7, 1998 (p. 1027).*
11. G.D. Chryssikos, E.I. Kamitsos, J.A. Kapoutsis, A.P. Patsis, V. Psyharis, A. Koufoudakis, Ch. Mitros, G. Kallias, E. Gamari-Seale, D. Niarchos, Physica C **254**, 44 (1995).
12. S.V. Bhat, in *Studies of High Temperature Superconductors*, Vol. **18** (Nova Science Publishers, New York, 1999), p. 241.
13. A.I. Smirnov, R.B. Clarkson, R.L. Belford, EPR Newslett. **11**, 9 (2000).
14. N. Guskos, V. Likodimos, M. Wabia, J. Typek, in *Symmetry and Pairing in Superconductors*, edited by M. Ausloos, S. Kruchinin (Kluwer Academic Publishers, 1999), p. 347.
15. P. Allenspach, A. Furrer, F. Hulliger, Phys. Rev. B **39**, 2226 (1989).
16. A.J. Kassman, J. Chem. Phys. **53**, 4118 (1970).
17. A. Furrer, P. Bruesch, P. Unternahrer, Phys. Rev. B **38**, 4616 (1988).
18. G.L. Goodman, C.-K. Loong, L. Soderholm, J. Phys. Cond. Matt. **3**, 49 (1991).
19. A.T. Boothroyd, S.M. Doyle, R. Osborn, Physica C **217**, 425 (1993).
20. L. Soderholm, C.-K. Loong, S. Kern, Phys. Rev. B **45**, 10062 (1992).
21. J. Mesot, P. Allenspach, U. Staub, A. Furrer, H. Mutka, R. Osborn, A.D. Taylor, Phys. Rev. B **47**, 6027 (1993).
22. V. Likodimos, N. Guskos, M. Wabia, J. Typek, Mol. Phys. Rep. **15/16**, 185 (1996).
23. M. Guillaume, P. Allenspach, J. Mesot, U. Staub, A. Furrer, R. Osborn, A.D. Taylor, F. Stucki, P. Unternahrer, Solid State Commun. **81**, 999 (1992).
24. V. Nekvasil, Solid State Commun. **65**, 1103 (1988).
25. B.G. Wybourne, J. Chem. Phys. **36**, 2301 (1962).
26. D. Barba, S. Jandl, V. Nekvasil, M. Marysko, M. Divis, A.A. Martin, C.T. Lin, M. Cardona, T. Wolf, Phys. Rev. B **63**, 054528 (2001).
27. A. Abragam, *The Principles of Nuclear Magnetism* (Clarendon Press, Oxford, 1961).
28. H. Mook, P. Dai, F. Dogan, Phys. Rev. B **64**, 012502 (2001).
29. M.V. Eremin, Yu. A. Sakhratov, A.V. Dooglav, I.R. Mukhamedshin, A.V. Egorov, JETP Lett. **73**, 540 (2001).
30. M. Eremin, A. Rigamonti, preprint, `xxx.lanl.gov/cond-mat/0103282`.